Supplement for: Time-resolved formation of excited atomic and molecular states in XUV-induced nanoplasmas in ammonia

R. Michiels,[1] A. C. LaForge,[1,2] M. Bohlen,[1] C. Callegari,[3] A. Clark,[4] A. von Conta,[5] M. Coreno,[6] M. Di Fraia,[7] M. Drabbels,[4] M. Huppert,[5] P. Finetti,[7] V. Oliver,[4] O. Plekan,[7] K. C. Prince,[7] S. Stranges,[8] V. Svoboda,[5] H. J. Wörner,[5] and F. Stienkemeier[1,9]

[1] *Institute of Physics, University of Freiburg, 79104 Freiburg, Germany*
[2] *Department of Physics, University of Connecticut, Storrs, Connecticut, 06269, USA*
[3] *Elettra-Sincrotrone Trieste S.C.p.A., 34149 Basovizza, Trieste, Italy*
[4] *Laboratory of Molecular Nanodynamics, Ecole Polytechnique Fédérale de Lausanne, 1015 Lausanne, Switzerland*
[5] *Laboratorium für Physikalische Chemie, ETH Zürich, 8093 Zürich, Switzerland*
[6] *ISM-CNR, Istituto di Struttura della Materia, LD2 Unit, 34149 Trieste, Italy*
[7] *Elettra-Sincrotrone Trieste, 34149 Basovizza, Trieste, Italy*
[8] *Department of Chemistry and Drug Technologies, University Sapienza, 00185 Rome, Italy, and Tasc IOM-CNR, Basovizza, Trieste, Italy*
[9] *Freiburg Institute of Advanced Studies (FRIAS), University of Freiburg, 79104 Freiburg, Germany*

(Dated: February 6, 2020)

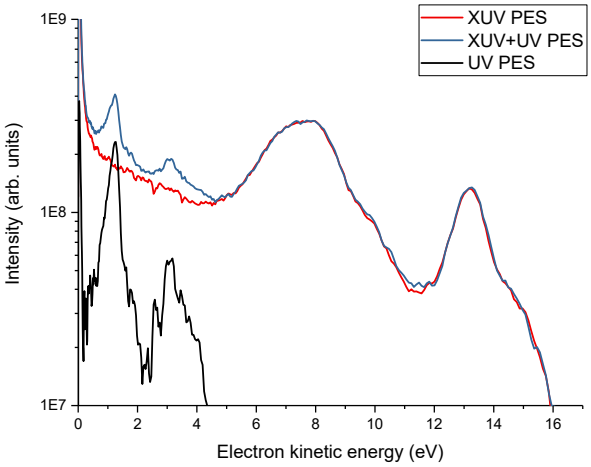

Figure 1. Photoelectron spectrum (PES) for XUV pump alone (red), XUV pump + UV probe (blue) and the difference between the former (UV-PES, black).

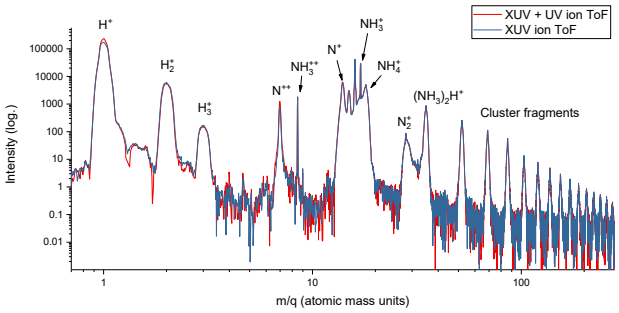

Figure 2. Ion time of flight spectrum (tof) for XUV pump alone and XUV pump + UV probe. The difference contains significant negative contributions and can not be shown in the log plot. A linear plot is shown in the manuscript in Fig.2 .

Analysis of XUV and XUV+UV photoelectrons and ions

The UV-photoelectron spectrum (UV-PES), also referred to as probe PES, was extracted by recording electron spectra in two operating modes, "XUV+UV" and "XUV only", which were run sequentially in alternation every 300 FEL shots, throughout the experiment. An exemplary PES of each mode is given in Fig. S1, along with the difference, the UV-PES. Varying the pump-probe delay between XUV and UV laser and subtracting gives the time-dependent probe ion and electron yields. The PES in Fig. S1 was recorded with 24.0 eV photon pulses from the FEL. At this photon energy, the two highest lying valence states of ammonia can be ionized and are visible as main contributions. The long low-energy tail of the photoelectron spectrum shows the large contributions of electrons emitted from the nanoplasma. The UV-PES, shown in black, makes up 5% to 10% of the total photoelectrons. A similar procedure was carried out for the ion time of flight spectra. The "XUV+UV" and "XUV only" ion tof is shown in Fig. S2. Protons are by far the most dominant contribution. Here too, the fraction of ions created by the UV probe laser is roughly 5% to 10% and dominated by the protons. The probe ions are shown in Fig. S3 and include positive and negative contributions. Negative probe yield indicates that the ion is depleted by the probe laser.

Time dependent probe ion yields for additional ions

These graphs show integrated probe ions versus pump-probe delay for the ionic fragments that are not shown in the manuscript. The uncertainty indicators are taken from the shot-to-shot fluctuation and show the

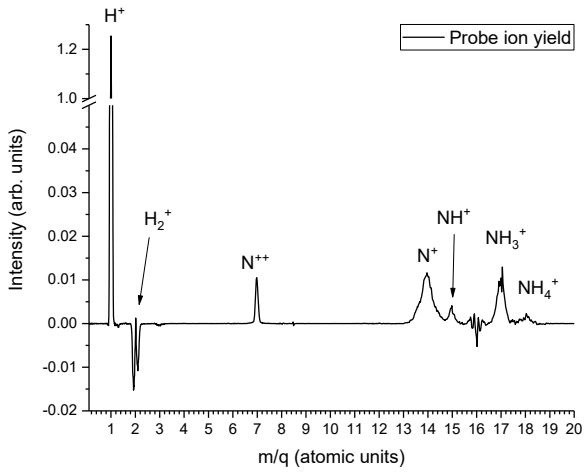

Figure 3. Difference between the XUV pump + UV probe and the XUV pump spectrum at a pump-probe delay of 18 ps. A negative yield shows that the ion signal is depleted by the probe laser.

statistical uncertainty of the data. Systematic errors are introduced in the subtraction procedure, which is explained in the first paragraph. They are in general reasonably compensated by normalizing the spectra to the overall intensity before subtracting. However, sometimes this cannot fully account for the observed fluctuations. Due to this, some of the data points show a large deviation from the general trend.

Determination of temporal overlap and t_0

The temporal overlap of the XUV and UV pulse was determined by two-photon resonant ionization of helium gas. The pump-probe dependent ion yield shows a FWHM width of roughly 200 fs. It is fitted with a cumulative normal distribution to determine t_0. The data and fit is shown in Fig. S7.

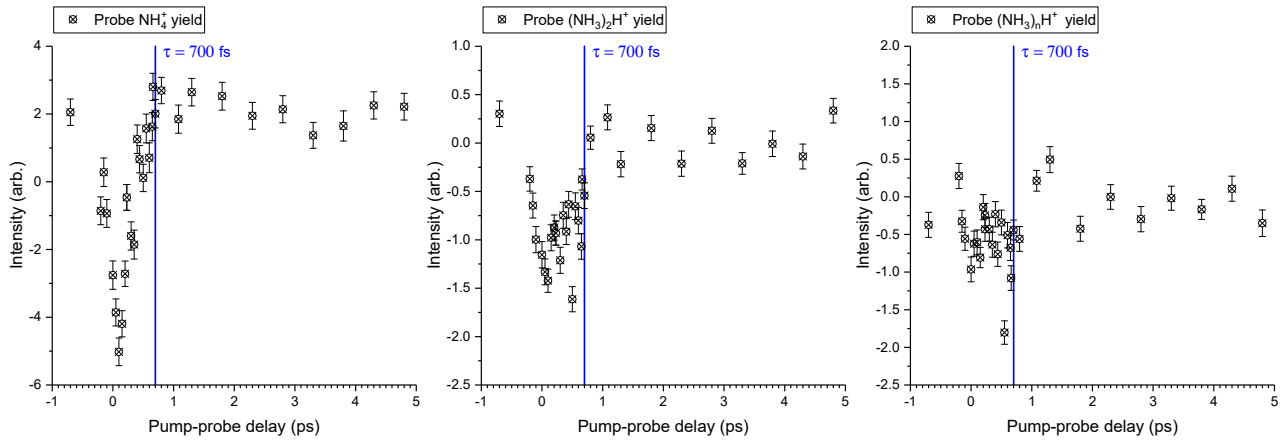

Figure 4. Time-dependent probe ion yield of the cluster fragments NH_4^+, the dimer, and larger fragments. Integrated ion yield is shown on the y-axis, pump-probe delay on the x-axis.

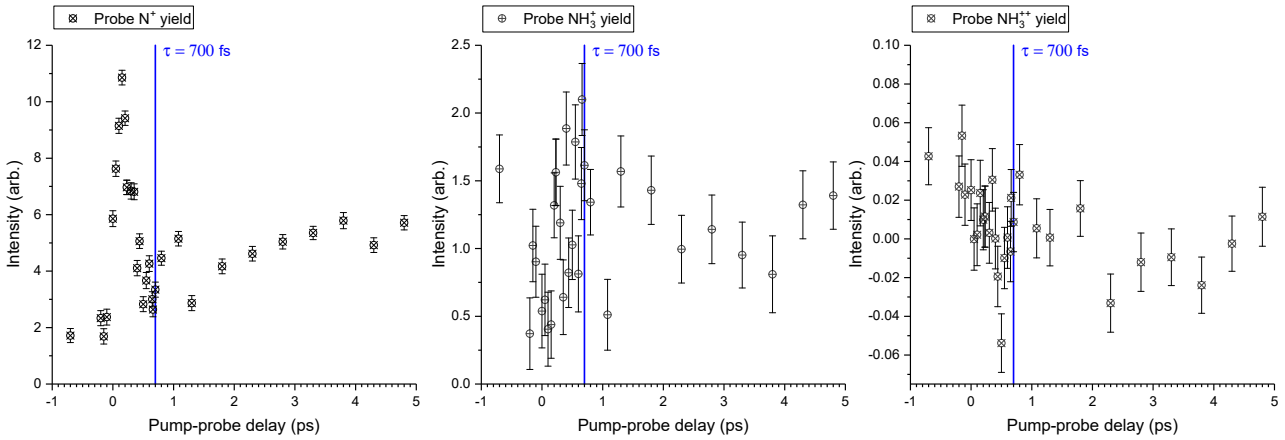

Figure 5. Time-dependent probe ion yield for N^+, NH_3^+, and NH_3^{++}. Integrated ion yield is shown on the y-axis, pump-probe delay on the x-axis.

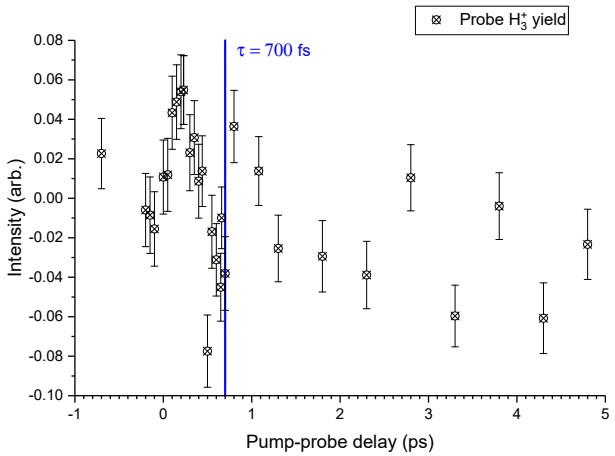

Figure 6. Time-dependent probe ion yield for H_3^+. Integrated ion yield is shown on the y-axis, pump-probe delay on the x-axis.

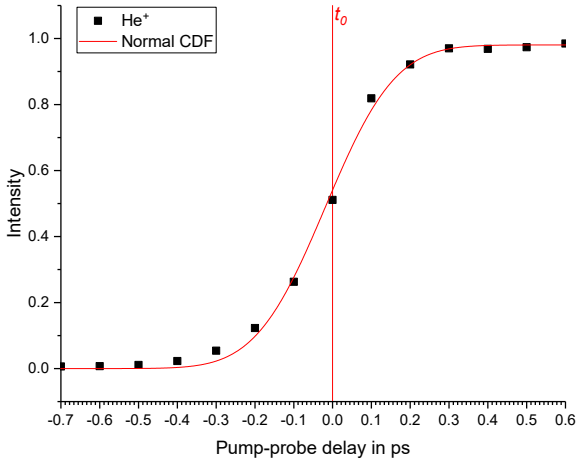

Figure 7. Time-dependent probe ion yield for H_3^+. Integrated ion yield is shown on the y-axis, pump-probe delay on the x-axis.